

Prediction of coronary artery plaque progression and potential rupture from 320-detector row prospectively ECG-gated single heart beat CT angiography: Lattice Boltzmann evaluation of endothelial shear stress

Frank J. Rybicki · Simone Melchionna · Dimitris Mitsouras · Ahmet U. Coskun · Amanda G. Whitmore · Michael Steigner · Leelakrishna Nallamshetty · Fredrick G. Welt · Massimo Bernaschi · Michelle Borkin · Joy Sircar · Efthimios Kaxiras · Sauro Succi · Peter H. Stone · Charles L. Feldman

Received: 5 November 2008 / Accepted: 29 December 2008
© Springer Science+Business Media, B.V. 2009

Abstract Advances in MDCT will extend coronary CTA beyond the morphology data provided by systems that use 64 or fewer detector rows. Newer coronary CTA technology such as prospective ECG-gating will also enable lower dose examinations. Since the current standard of care for coronary diagnoses is catheterization, CT will continue to be benchmarked against catheterization reference points, in particular temporal resolution, spatial resolution,

radiation dose, and volume coverage. This article focuses on single heart beat cardiac acquisitions enabled by 320-detector row CT. Imaging with this system can now be performed with patient radiation doses comparable to catheterization. The high image quality, excellent contrast opacification, and absence of stair-step artifact provide the potential to evaluate endothelial shear stress (ESS) noninvasively with CT. Low ESS is known to lead to the development and

F. J. Rybicki (✉) · D. Mitsouras · A. G. Whitmore · M. Steigner · L. Nallamshetty
Applied Imaging Science Laboratory, Department of Radiology, Brigham and Women's Hospital, Harvard Medical School, 75 Francis Street, Boston, MA 02115, USA
e-mail: frybicki@partners.org

F. J. Rybicki · M. Steigner · L. Nallamshetty
Noninvasive Cardiovascular Imaging, Department of Radiology, Brigham and Women's Hospital, Harvard Medical School, Boston, MA, USA

S. Melchionna · M. Borkin
Department of Physics, Harvard University, Cambridge, MA, USA

S. Melchionna · M. Borkin · J. Sircar · E. Kaxiras
School of Engineering and Applied Science, Harvard University, Cambridge, MA, USA

S. Melchionna
Department of Physics, University of Rome La Sapienza, Rome, Italy

S. Melchionna
INFN-CNR, Rome, Italy

A. U. Coskun · F. G. Welt · P. H. Stone · C. L. Feldman
Cardiovascular Division, Department of Medicine, Brigham and Women's Hospital, Harvard Medical School, Boston, MA, USA

A. U. Coskun
Mechanical and Industrial Engineering,
Northeastern University, Boston, MA, USA

M. Bernaschi · S. Succi
Istituto Applicazioni Calcolo, CNR, Rome, Italy

S. Succi
Initiative in Innovative Computing, Harvard University, Cambridge, MA, USA

progression of atherosclerotic plaque culminating in high-risk vulnerable plaque likely to rupture and cause an acute coronary event. The magnitude of local low ESS, in combination with the local remodeling response and the severity of systemic risk factors, determines the natural history of each plaque. This paper describes the steps required to derive an ESS map from 320-detector row CT data using the Lattice Boltzmann method to include the complex geometry of the coronary arterial tree. This approach diminishes the limitations of other computational fluid dynamics methods to properly evaluate multiple coronary arteries, including the complex geometry of coronary bifurcations where lesions tend to develop.

Keywords Computed tomography · Shear stress · Atherosclerosis · Coronary disease · Vascular remodeling

Introduction

Multi-detector computed tomography (MDCT) is an emerging modality for coronary artery imaging because it has potential to assess the coronary artery lumen, the wall, and plaque. MDCT does not use catheterization and is potentially suitable for serial evaluations over time. Earlier generations of MDCT, such as 16-detector row CT, were limited by excessive radiation exposure, data acquisition that required prolonged breath-holding, and artifacts that limited precise characterization of coronary artery morphology. The transition from 16- to 64-slice coronary CT improved spatial resolution, temporal resolution, and volume coverage per gantry rotation. These advances made cardiac CT a more robust tool for clinical use and for innovative diagnostic approaches. One significant problem in defining clinical algorithms for cardiac CT is that the technology developments outpace the accumulation of large patient series to perform studies. However, it is generally accepted that 64-slice CT has a very high negative predictive value and can be used to exclude coronary artery disease (CAD) in low- and intermediate-risk patients. In addition, CT is recognized as not only much simpler to perform than coronary catheterization, but also as an exam with fewer complications.

As CT of the heart has expanded beyond 64-detector rows, further innovations have become available,

including the use of MDCT to characterize coronary artery plaque and the local coronary artery hemodynamic environment in a precise, 3-dimensional manner to identify specific areas of plaque formation and to predict the nature of future progression. Early identification of high-risk vulnerable plaque would be invaluable since such prognostic information would allow for risk-stratification of individual coronary lesions and application of highly selective interventions to areas likely to cause a new cardiac event. The purpose of this review is to describe 320-detector row CT as a new tool to explore a potentially revolutionary application intended to predict the natural history of individual coronary atherosclerotic plaques.

Lower dose cardiac MDCT

Until recently, state-of-the-art noninvasive coronary CT acquisitions used 64-slice technology, either from 64-detector rows or 32-detector rows and an alternating X-ray focal spot. One criticism of 64-slice cardiac CT has been patient radiation, since the dose delivered by CT has been higher than that obtained with diagnostic catheterization. To lower radiation dose, contemporary cardiac CT protocols have migrated from retrospective ECG gating where radiation dose is delivered throughout the cardiac cycle to prospective ECG gating for which data is acquired, and therefore radiation dose is delivered, only within a pre-determined “phase window” of the R–R interval. When prospective ECG gating is used, no CT data is acquired for most of the cardiac cycle. Thus, cine evaluation of the myocardium and valves is not available. However, as the phase window is narrowed, cardiac CT doses become comparable to those of diagnostic cardiac catheterization. The optimum width of the phase window for prospectively ECG gated CT depends on patient and hardware considerations; this is an active area of investigation. However, by narrowing the phase window and judiciously choosing the mA and kV settings for image acquisition, very low dose cardiac CT data sets can be achieved.

The increased volume coverage per gantry rotation in MDCT has revolutionized the imaging of many body parts, including the heart. This review focuses on 320 × 0.5 mm detector row (Toshiba AquilionONE Dynamic Volume CT, Tochigi-ken, Japan) coronary CTA with 16 cm of craniocaudal coverage

per gantry rotation that achieves single R–R, or single heart beat, cardiac imaging. In addition to the faster overall CT acquisition from 320-detector rows, whole cardiac volumes acquired with this technology implicitly eliminate “stair-step” artifacts inherent in sub-volume CT where data for each sub-volume are acquired over multiple gantry rotations and the sub-volumes, or slabs, are stacked to complete the cardiac volume. Another benefit of 320-detector row technology is that the single R–R acquisition captures the state of the entire iodinated contrast enhanced coronary circulation at a single time point, mitigating the differences in opacification that are inevitable with sub-volume coronary CTA. The result is uniform cardiac data sets that are highly amenable to advanced analyzes. An innovative application of this enhanced methodology focuses on the noninvasive evaluation of coronary artery endothelial shear stress (ESS) with the goal of achieving noninvasive coronary vascular profiling as an adjunct to the standard morphology data from cardiac CT. Data concerning plaque morphology and the hemodynamic environment in which the plaque is located can be used to then predict the development of high-risk plaque likely to progress to plaque rupture and precipitation of an acute clinical coronary event.

Pathobiological role of local coronary ESS in the development and progression of CAD and vulnerable plaque

Atherosclerosis is a chronic, inflammatory, fibroproliferative disease primarily of large and medium-sized conduit arteries. Although the entire coronary circulation is exposed to systemic risk factors, coronary atherosclerotic lesions primarily form where there is disturbed coronary flow, specifically bifurcations such as the branch point of the left anterior descending and left circumflex arteries [1, 2]. These focal lesions result primarily from hemodynamic forces, with ESS playing the most fundamental role [3].

Low ESS modulates endothelial gene expression, inducing an atherogenic endothelial phenotype and formation of an early atherosclerotic plaque [3]. In arterial regions with disturbed flow, low ESS reduces the bioavailability of nitric oxide, while upregulating potent vasoconstrictive and mitogenic molecules, thereby inducing endothelial dysfunction and

exposing the endothelium to the atherogenic effect of local and systemic risk factors. Low ESS also promotes low-density lipoprotein-cholesterol (LDL-C) uptake and mediates the production of reactive oxygen species (ROS) within the intima. Low ESS also downregulates the intracellular ROS scavengers, further augmenting local oxidative stress [3].

Through activation of nuclear factor- κ B, low ESS upregulates the expression of several adhesion molecules, chemoattractant chemokines, and pro-inflammatory cytokines [3]. Once monocytes infiltrate beneath the endothelium, they undergo structural and functional alterations and differentiate to macrophages, which express scavenger receptors, phagocytize the oxidized LDL-C and transform to foam cells. Foam cells produce cytokines, growth factors, ROS and matrix degrading enzymes, sustaining the local inflammation, oxidative stress, dynamic matrix remodeling, and ultimately atherosclerosis progression. Overexpression and increased activity of matrix metalloproteinases and cathepsins, which are the major proteases associated with extracellular matrix (ECM) degradation, are also mediated directly by low ESS [4–6].

As plaques progress, the regional disruption of the internal elastic lamina (IEL), which separates the diseased intima from the media, constitutes the key event that drives the formation of fibroatheromas [4]. In the setting of very low levels of local ESS, and subsequently intense accumulation of inflammatory cells within the intima, the part of the IEL beneath the plaque undergoes local degradation by the foam cells-derived proteases [4]. These IEL breaks constitute the gateway for vascular smooth muscle cells (VSMCs), which are originally located into the media, to enter the intima. Within the intima the VSMCs differentiate to a more synthetic phenotype to elaborate ECM proteins (e.g. collagen and elastin), thereby promoting plaque progression. The VSMCs encompass the core of the lipid-laden foam cells (lipid core), produce ECM and create the fibrous cap, separating the thrombogenic lipid material from the circulating platelets and other pro-thrombotic factors.

The natural history of each early plaque is dependent not only on the formation and progression of atherosclerosis, but also on the vascular remodeling response [7–10]. If the local ESS environment is initially low, atherogenic factors predominate and a proliferative plaque will form. If the local ESS is

sufficiently low, or evolves to a sufficiently low value, then inflammatory processes will coexist with the proliferative phenotype, leading to degradation of the extracellular matrix and, consequently, to local expansive vascular remodeling which in turn leads to an even lower local ESS [4]. This progressively lower ESS further exacerbates the pro-inflammatory and pro-atherogenic stimuli of the local plaque, creating a vicious cycle of low ESS, progressively more intense inflammation and lipid accumulation, and even lower ESS. This process culminates in the formation of the so-called “vulnerable plaque” characterized by a large extracellular lipid pool with a necrotic core and a thin fibrous cap in the setting of a locally expansively remodeled artery [3]. This vulnerable plaque, which is prone to rupture with superimposed thrombus

formation, is the high-risk substrate from which the majority of acute coronary syndromes originate (Fig. 1). The vast majority of these inflamed high-risk vulnerable plaques do not encroach significantly into the coronary artery lumen, do not limit coronary blood flow, and can not be detected by myocardial perfusion imaging.

The marked heterogeneity of natural history trajectories of coronary plaque lends itself to development of a comprehensive risk stratification approach to characterize each individual plaque at an early stage [3]. Since the driving factor for ongoing plaque proliferation, lipid accumulation, and intense inflammation is the magnitude of local low ESS and the presence of expansive remodeling, measurement of these characteristics in vivo should

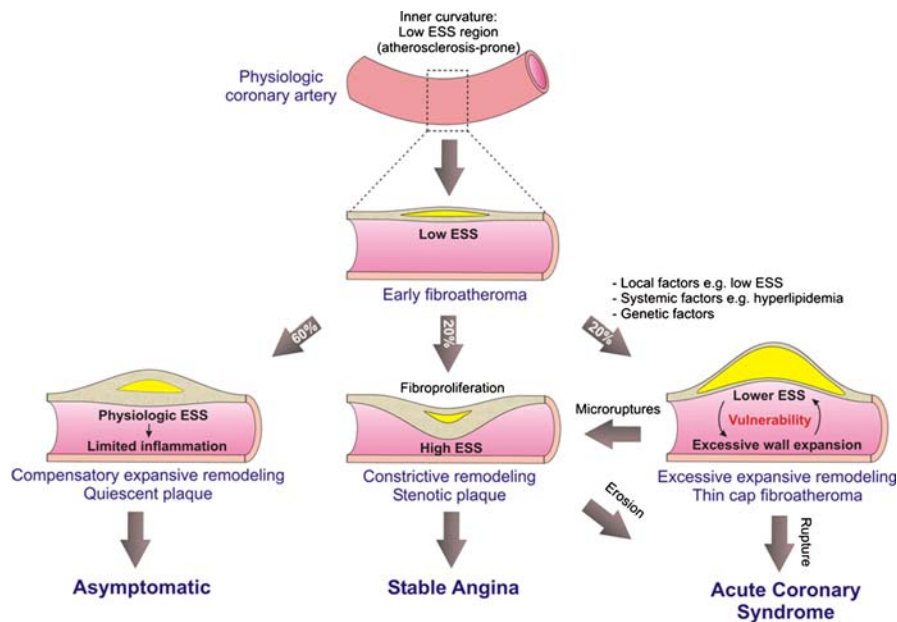


Fig. 1 Proposed natural history of coronary atherosclerosis and opportunity for pre-emptive intervention. The initiating process of atherosclerosis in an atherosclerosis-prone host is a low ESS environment, leading to the formation of an early fibroatheroma, which may be diffuse. The vascular response to that early fibroatheroma likely determines the nature of the subsequent natural history of that plaque. If there is local compensatory expansive remodeling, then the local ESS is normalized, the hemodynamic stimulus for further plaque progression is resolved, and the early lesion evolves to a quiescent plaque with limited inflammation. However, in the presence of certain local, systemic, and genetic factors, the local vascular wall may undergo excessive expansive remodeling. In this context the local low ESS environment persists, promoting further plaque progression and vessel expansion. A self-

perpetuating vicious cycle is established among local low ESS, excessive expansive remodeling and plaque inflammation, transforming the early fibroatheroma to a thin cap fibroatheroma. The stenotic plaques may either evolve with a phenotype promoting fibroproliferation consistently throughout their natural history course, or may represent an end-stage of scarring in the setting of prior inflamed thin cap fibroatheroma through repetitive microruptures and healing. Also, the stenotic plaques may infrequently undergo local erosion or develop calcified nodules, and lead to local thrombus formation and manifestation of an acute coronary syndrome. The percentages reported in the figure are based on IVUS studies. In vivo identification of the natural history course of each individual coronary artery plaque may allow for pre-emptive intervention to avert an adverse cardiac event. Figure used with permission from [3]

enable risk stratification for the entire coronary circulation.

Vascular profiling methodology to characterize local ESS and vascular remodeling

The most comprehensive technique for investigating the relationship between ESS and vascular pathobiology is a methodology known as vascular profiling that, to date, utilizes intravascular ultrasound (IVUS) and coronary angiography to create an accurate 3D representation of both the lumen and external elastic membrane (EEM) of individual coronary arteries [11]. ESS is then derived by numerically solving the basic equations of fluid mechanics within this 3D representation of the artery while remodeling characteristics are derived from changes in the dimensions of lumen and EEM. Vascular profiling is accurate and highly reproducible [11], and can be used to track changes in lumen, wall thickness, and ESS in periods as short as 6–9 months in humans or experimental animals [4, 12, 13]. A natural history clinical study (PREDICTION Trial) of atherosclerotic plaques using catheterization and IVUS vascular profiling techniques in patients with coronary artery disease is now underway to determine the incremental value of characterizing the local ESS and remodeling environment to predict the development of new acute cardiac events.

Our new ability to noninvasively image the entire coronary arterial tree in a single heart beat has sparked a new investigation of CT vascular profiling described in this article. To date, the major limitation of determining ESS maps and correlating these findings with the location of future cardiac events and, ultimately, patient outcomes has been the difficulty and risk associated with IVUS. However, MDCT technology makes these analyses feasible in a noninvasive manner. In the subsequent section we describe the methods, via an example case, of 320-detector row Dynamic Volume CT vascular profiling. We highlight the strengths and weaknesses of this approach, and the uniqueness of low-dose, prospectively ECG-gated wide area detector CT for this new application that extends the current evaluation of the coronary arteries beyond the morphology data that is now routinely obtained. We then describe our strategy to validate this approach in a small series of

patients who will also undergo the more traditional vascular profiling using IVUS. Finally, we outline a method to further validate 320-detector row CT vascular profiling role using data from multiple institutions.

320-detector row dynamic volume CT for vascular profiling to predict localization of high-risk coronary plaque responsible for new coronary events

Acquisition of CT images

Patients scheduled to undergo CT vascular profiling are imaged axially using a 320×0.5 mm detector configuration scanner with a rotation time of 350 ms. The standard cardiac CT protocol uses 120 kV, although 100 kV can be used in smaller patients to decrease patient radiation. The typical mA = 400, although higher settings, up to 580 with this CT unit, can be used for larger patients. Prospective ECG gating is used to lower radiation dose; the standard width of the phase window is 10% (70–80% R–R). All patients receive 80 ml of iopamidol 370 mg I/ml (Isovue-370, Bracco Diagnostics, Princeton, NJ) followed by 40 ml normal saline injected with a dual injector (EZEM Empower CTA DUAL Injector, EZEM Inc., Lake Success, NY) at 6 ml/s. In the typical protocol for coronary CTA, bolus tracking in the descending aorta is performed using a 200 Hounsfield unit (HU) threshold and a single data set is acquired. This does not provide information regarding coronary blood flow that is needed for ESS. For IVUS vascular profiling, contrast is tracked as it fills the known arterial volume. The coronary blood flow rate is simply the volume of the artery between two points divided by the time for contrast opacification of that volume. Using multiple whole heart acquisitions, data can be acquired to estimate coronary blood flow. Since this requires multiple CT acquisitions, those not used for coronary anatomy can be obtained at lower radiation levels by decreasing the mA, kVP, or both.

All patients with a resting heart rate greater than 65 beats per minute receive intravenous metoprolol in 5 mg increments; patients imaged with a lower heart rate have more cardiac phases considered to be of excellent image quality [14]. All patients receive

0.4 mg sublingual nitroglycerine before imaging. For each patient, the reconstruction phase with minimum artifact is determined at the CT console, and this data set is transferred to a research image post-processing workstation (Vitrea 4.0, Vital Images, Minnetonka, MN, USA).

Computational fluid dynamics: Navier–Stokes single vessel profiling versus Lattice Boltzmann methods for vascular profiling

Computation of the flow patterns with the reconstructed coronary artery lumen has traditionally relied on numerical solutions to the Navier–Stokes equations of fluid mechanics. These currently available methods of CFD require that the volume under investigation be divided into small voxels and that the laws of motion and of conservation of mass are satisfied for each voxel. Using this method, typical solutions have 1,920 voxels per millimeter of coronary artery and have proven to be computationally efficient and sufficiently realistic to accurately predict regions of accelerated atherosclerosis and increased inflammation. When using IVUS data, this approach has an important limitation that only one vessel can be analyzed; branches and bifurcations cannot be reconstructed and, as a result, are ignored. However, 320-detector row CT yields a high image quality [15], single heart beat, whole volume representation of the coronary arterial system, including the complex geometries of coronary bifurcations. When applied to CT data, another limitation of conventional CFD methods is that the coronary branching results in an impractical computational burden.

In order to compute flow patterns within a complex CT volumetric representation of the coronary arteries, have adopted the Lattice Boltzmann method [16] rather than the discretization inherent in the Navier–Stokes equations. In the Lattice Boltzmann method, the volume under consideration (typically either the left or the right coronary artery system) is filled with a rectangular array of lattice points and a form of the classical Boltzmann equation of kinetic theory is simultaneously solved for each lattice point. Although the present Lattice Boltzmann method to deduce ESS is computationally demanding, it has distinct advantages. As noted above, it enables analyzes of a very complex and complete coronary anatomy. Second, the Lattice Boltzmann

method can be easily adapted to run on computers that consist of a very large number of inexpensive processors, all operating in parallel. Our results were obtained using a 1,024 node portion of an IBM Blue Gene supercomputer.

As discussed in greater detail below, the long term goal of 320-detector row CT vascular profiling is integration to the CT console. Thus, vast computation would be considered a relative limitation of this technique. However, we have recently adapted the Lattice Boltzmann method code to run on a conventional graphics processing unit [17]; thus the computational burden of coronary vascular profiling is considered feasible within the hardware configuration that could be available in future generation CT scanners.

Luminal volume geometry extraction

Because of the complex course and branching of the coronary arteries, cardiac CT interpretation requires advanced image reformation. Such post-processing tools already include coronary artery segmentation algorithms to assist in the evaluation of lesions. At present, commercially available software can provide fully, or nearly fully, automated segmentation methods based on HU differences (Fig. 2a).

Work in this project used a research build of the Vitrea 4.0 workstation that exports the geometry of the luminal volume, as determined by the built-in segmentation algorithm, into a data file. This geometric “mesh” consists of a set of 3D Cartesian coordinates enclosing the volume of the coronary lumens (Fig. 3a). For this model, all major coronary arteries plus all branches greater than 1 mm in diameter were included. In clinical practice, manual adjustment of the lumen center line is occasionally required and is fully supported by the software. However, additional manipulation was not required in this case because of the excellent iodinated contrast opacification, lack of cardiac motion on the best phase obtained, and inherent absence of stair-step artifact in 320-detector row cardiac CT.

For this example, the mesh reflected the coordinates of the outer surface of the segmented endoluminal volume at an angular resolution of 1.4° at each selected cross-section, orthogonal to the center line. Cross-sections were obtained every 0.5 mm. In IVUS based vascular profiling, the computational grid

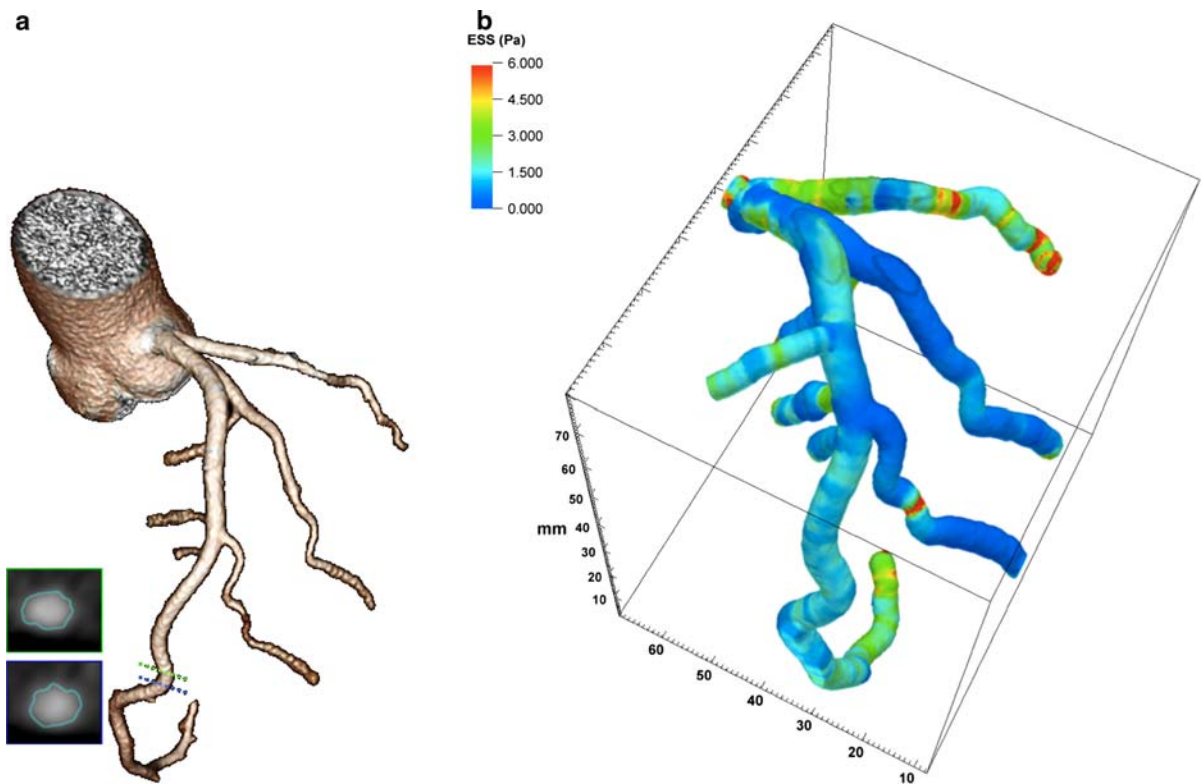


Fig. 2 Left coronary system in a patient imaged with 320-detector row coronary CTA. **a** Automatically segmented coronary arteries and branches with lumen greater than or equal to 1 mm are illustrated. **b** Corresponding endothelial

shear stress vascular profiling of the same coronary tree using Lattice Boltzman code. *Color shading* shows the ESS values reflected on the lumen surface, with *blue* depicting low ESS and *red* depicting high ESS

describing the volume enclosed by the surface mesh is generated at an angular resolution of 11.25° . The resolution of the 320-detector row CT derived mesh was reduced to this requirement in conjunction with low-pass filtering using a Gaussian filter with standard deviation equal to 3° along the cross-section, and 0.5 mm longitudinally (Fig. 3b). This was also desirable because it reduced small-scale irregularities in the segmented surface. Such irregularities in the anatomy of the lumen are inherently introduced by the segmentation process due to the noise of the physical imaging system.

A different computational grid is required to describe the volume enclosed by the lumen for Navier–Stokes CFD and the Lattice Boltzmann approaches. The left panel of Fig. 4 presents the 3D Cartesian computational grid used with Lattice Boltzmann methods. The spacing of the grid points is $20\ \mu\text{m}$ in order to sufficiently capture the complex 3D geometry of the branching vessels. Computations

are performed at each grid point. The right panel of Fig. 4 presents the unstructured grid that is typically used for Navier–Stokes CFD methods; computations are performed within each voxel. Voxels are coarser near the center of the vessel, and reach a radial resolution of $20\ \mu\text{m}$ at the lumen.

Examples of 320-detector row dynamic volume coronary CT vascular profiling

To validate the current version of the Lattice Boltzmann Code, a 6 cm length of a human right coronary artery for which a prior CFD solution had already existed was reanalyzed using the MUPHY Lattice Boltzmann code outlined above. The previously measured coronary flow rate was 1.38 ml/s. To assure maximum accuracy, the Lattice Boltzmann lattice points were positioned on a 3D Cartesian grid at even intervals of $20\ \mu\text{m}$ and the code was run on 1,024 nodes of a Blue Gene supercomputer.

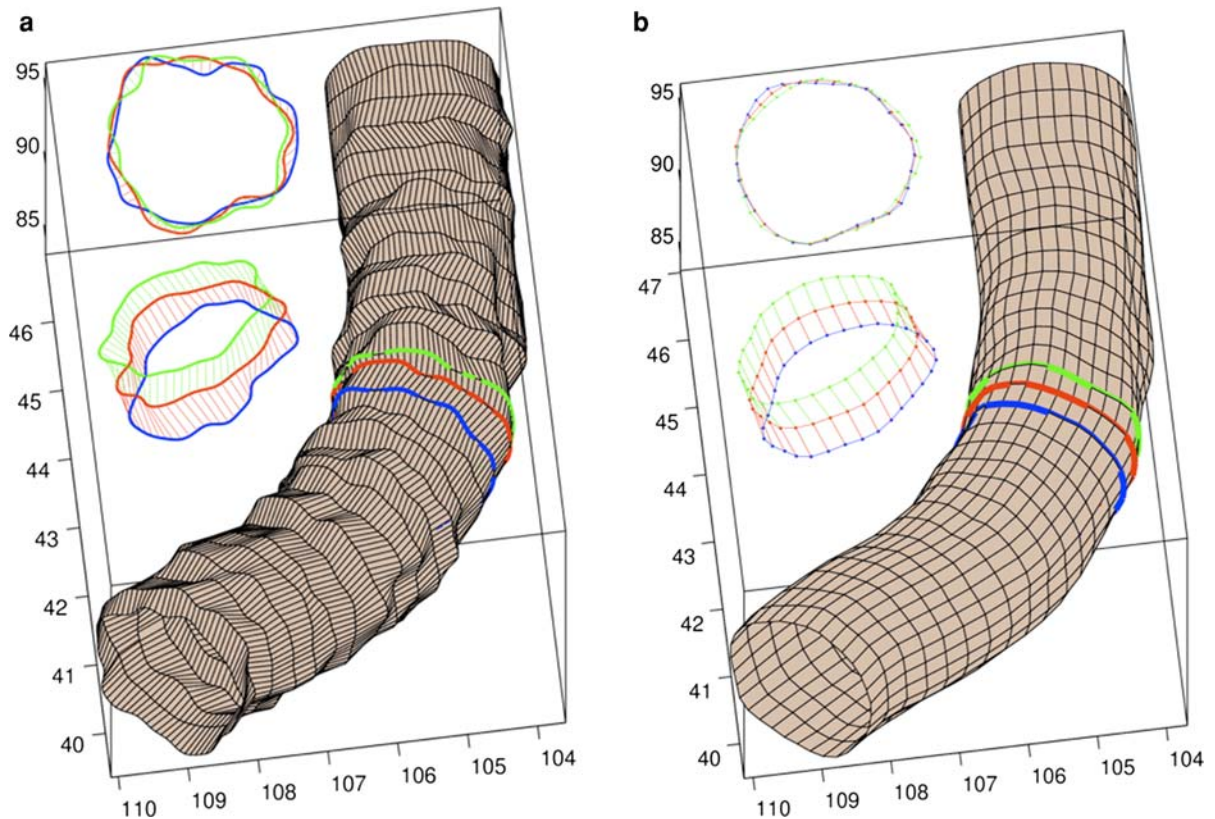
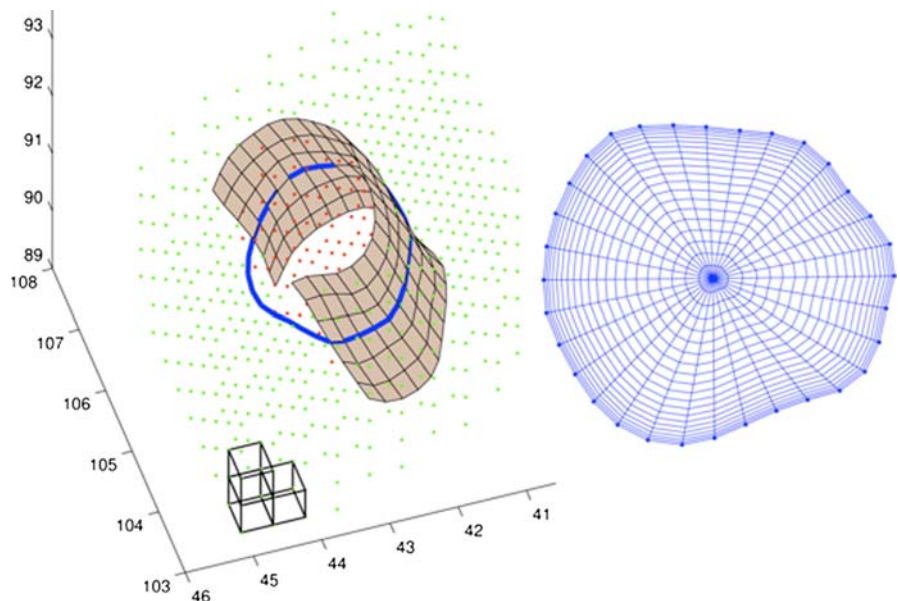


Fig. 3 Three-dimensional grid for ESS calculations. **a** automatically detected lumen surface over a segment of the LAD, *inset* shows the geometric mesh for three consecutive slices along the center line (*top inset*) and at an arbitrary angle

(*bottom inset*). **b** revised grid of the same left anterior descending segment after low-pass filtering and subsampling as described in the text. *Inset* shows same three slices as in (a)

Fig. 4 Computational grids used by the Lattice Boltzmann (*left panel*) and Navier–Stokes CFD methods (*right panel*). For Lattice Boltzmann, computations are performed at every 3D Cartesian grid point within the lumen (*red-colored points*); grid spacing is $20\ \mu\text{m}$ (not shown to scale for clarity). For Navier–Stokes CFD, computations are performed within voxels determined by 20 radial and 32 angular subdivisions of the volume enclosed by each cross-section. The radial resolution is lower near the centerline and reaches $20\ \mu\text{m}$ at the lumen



The results of the validation study showed very similar patterns using either Navier–Stokes solution with Phoenix CFD or Lattice Boltzmann solution with MUPHY code (Fig. 5). ESS for each solution varied from approximately 1 to 6 Pa. The maxima and minima occurred at the same locations on the coronary artery with either method, and the qualitative appearances of the two solutions were essentially identical. A slightly greater asymmetry in the ESS pattern of the Lattice Boltzmann solution was observed but is attributable to the use of a slightly different inlet velocity distribution. Computation time of the Phoenix code running on a high end single processor PC was approximately 12 min; computation time of the Lattice Boltzmann code was approximately 1 h.

Figure 2b illustrates the Lattice Boltzmann based 320-detector row MDCT profiling of the entire left coronary system. Subtle variations of ESS from the inner surface to the outer surface of bends and in the regions of branching are clearly visible. ESS values are generally in the physiological range (1.5–5.0 Pa) with a few areas being lower than normal. Producing this ESS map for the entire left coronary system required approximately 1 day of computation time.

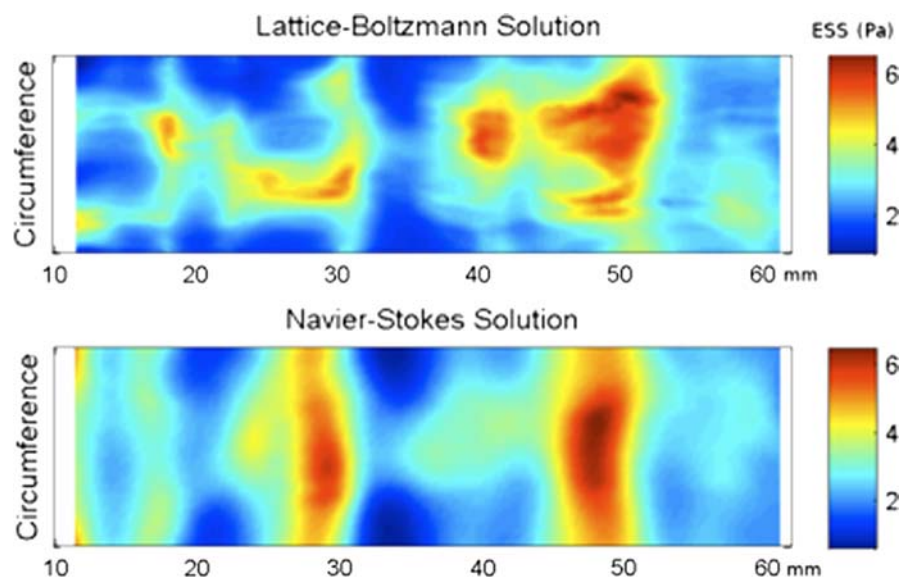
As noted above, we implemented the Lattice Boltzmann technique for hemodynamic analysis because of the complexity of the coronary anatomy that can be studied in one heart beat with 320-detector row CT. Conventional Navier–Stokes based CFD solvers have been in existence for many decades, none

of the grid formation systems is readily adaptable to represent the complexity of coronary CTA images while still maintaining computational efficiency. Conversely, the Lattice Boltzmann technique, a computationally more demanding system, was developed to model very complex structures. Accordingly, the creation of a Lattice Boltzmann grid is typically very simple and is usually performed automatically. We completed the Lattice Boltzmann calculations (Fig. 2b) on a portion of a very large supercomputer—a computer that is much too large and expensive to be used for routine coronary CTA. Our choice of the Blue Gene was largely dictated by its ready accessibility and cost-free access. An additional reason to use this massively parallel supercomputer is that our code can be readily formatted to run on a parallel computer with essentially no loss in efficiency. We have also ported the Lattice Boltzmann code to run on the latest, very small, highly parallel version of an inexpensive game-oriented computer. This will soon be available to compute ESS maps quickly and efficiently, in keeping with the long-term goal of obtaining such data from the CT console.

Potential limitations and challenges to performing vascular profiling with MDCT

Unlike ESS maps obtained from IVUS, CT vascular profiling has not yet been demonstrated to be

Fig. 5 Comparison of ESS patterns computed using Lattice Boltzmann (*top*) and Navier–Stokes (*bottom*) CFD methods. A pathology view is presented, where the vessel is unrolled along its length. Computation was based on the lumen geometry obtained via IVUS vascular profiling of a human right coronary artery. ESS maxima and minima occur at the same locations with either method



reproducible. Thus, the next validation step for this work is a study of patients who undergo vascular profiling with both 320-detector row CT and IVUS. Initial results from this investigation are encouraging, but there are limitations. For example, IVUS has superior spatial resolution when compared to CT. The resolution of IVUS is approximately $100\ \mu$ both axially and radially. For current vascular profiling, the axial resolution is degraded to approximately $400\ \mu$ because samples are obtained only at end-diastole. Thus, the axial resolution is comparable to the 350 micron isotropic resolution of 320-detector row CT. One goal of the next validation step is to evaluate the impact of a different radial resolution ($100\ \mu$ for IVUS vs. 350 for CT) to sufficiently characterize coronary morphology so that CT vascular profiling maps approximate those obtained by IVUS. In addition, the more traditional vascular profiling data acquisition uses either a modified TIMI frame count method [18] or a flow wire method to determine coronary blood flow. The direct flow wire measurement is not available for coronary CT profiling. Thus, estimates of coronary blood flow must be used in the ESS algorithm. This can be done with a library of cases developed from the PREDICTION trial. In addition, it may be possible to estimate coronary blood flow from images data obtained from the iodinated contrast media bolus tracking method, somewhat similar to the modified TIMI frame count method.

For longer term validation, MDCT in general is challenged in that multi-center trials are difficult to perform since the technology continues to outpace the ability to obtain sufficient data. To date, there are two multi-center 64-detector row MDCT trials that have been presented in a peer-review format. The Core64 trial [19] focused on primarily teaching hospital patients. This study of 291 patients used receiver operating characteristic analysis to demonstrate that 64-detector row coronary CTA was equivalent to quantitative coronary angiography for the prediction of the need for revascularization. Patients studied in the ACCURACY trial [20] were recruited from 16 United States private practice centers and showed, using a different 64-detector row coronary CTA platform, a sensitivity = 91%, specificity = 84%, positive predictive value = 51%, and negative predictive value = 98%. It is also important to note that neither of these trials includes long-term follow-up for which events predicted by CT are

correlated with patient outcomes. At present, a 320-detector row CT multi-center trial is being planned with long-term patient follow-up that will be required to validate vascular profiling.

Conclusions

The goal of vascular profiling is risk stratification of individual coronary plaques that extends beyond the morphology data now available from standard coronary CTA. In vivo understanding of the local hemodynamic environment responsible for future behavior of individual plaques, when combined with current data already available, could lead to more accurate risk stratification of individual lesions. Thus, a plaque that is identified as “high-risk” of rupturing and causing an acute coronary syndrome in a patient with other risk factors could undergo intensive, selective therapeutic intervention including, in some cases, placement of a coronary stent or local drug delivery. Such prophylactic or pre-emptive focal treatment strategies would be based on the likelihood of the inflamed vulnerable plaque to rupture, even in the absence of an associated limitation in coronary blood flow. The potential clinical and economic implications of identifying and treating individual high-risk, non-flow-limiting coronary lesions are enormous.

In summary, coronary artery segments in a low ESS environment are more likely to develop early atherosclerotic plaque, and the persistence of low and very low ESS states induces differentiation to high-risk plaques. The methods of vascular profiling, currently performed with IVUS, accurately and reproducibly determine coronary ESS and can predict those lesions that are more likely to cause clinical events. Three-hundred twenty detector row CT has the potential to noninvasively yield equivalent information and dramatically expand the application of coronary vascular profiling. This work demonstrates the feasibility of profiling and highlights the benefits of 320-detector row CT for this application. Future validation and implementation steps are needed to further understand plaque characteristics, local ESS, and the vascular remodeling response for the population of patients undergoing advanced coronary CTA.

Acknowledgment This work is supported by a grant to Dr. Rybicki from Toshiba Medical Systems Corporation.

References

1. Malek AM, Alper SL, Izumo S (1999) Hemodynamic shear stress and its role in atherosclerosis. *JAMA* 282:2035–2042. doi:[10.1001/jama.282.21.2035](https://doi.org/10.1001/jama.282.21.2035)
2. Asakura T, Karino T (1990) Flow patterns and spatial distribution of atherosclerotic lesions in human coronary arteries. *Circ Res* 66:1045–1066
3. Chatzizisis YS, Coskun AU, Jonas M et al (2007) Role of endothelial shear stress in the natural history of coronary atherosclerosis and vascular remodeling: molecular, cellular, and vascular behavior. *J Am Coll Cardiol* 49:2379–2393. doi:[10.1016/j.jacc.2007.02.059](https://doi.org/10.1016/j.jacc.2007.02.059)
4. Chatzizisis YS, Jonas M, Coskun AU et al (2008) Prediction of the localization of high-risk coronary atherosclerotic plaques on the basis of low endothelial shear stress: an intravascular ultrasound and histopathology natural history study. *Circulation* 117:993–1002. doi:[10.1161/CIRCULATIONAHA.107.695254](https://doi.org/10.1161/CIRCULATIONAHA.107.695254)
5. Galis ZS, Sukhova GK, Lark MW et al (1994) Increased expression of matrix metalloproteinases and matrix degrading activity in vulnerable regions of human atherosclerotic plaques. *J Clin Invest* 94:2493–2503. doi:[10.1172/JCI117619](https://doi.org/10.1172/JCI117619)
6. Galis ZS, Khatri JJ (2002) Matrix metalloproteinases in vascular remodeling and atherogenesis: the good, the bad, and the ugly. *Circ Res* 90:251–262
7. Feldman CL, Coskun AU, Yeghiazarians Y et al (2006) Remodeling characteristics of minimally diseased coronary arteries are consistent along the length of the artery. *Am J Cardiol* 97:13–16. doi:[10.1016/j.amjcard.2005.07.121](https://doi.org/10.1016/j.amjcard.2005.07.121)
8. Nakamura M, Nishikawa H, Mukai S et al (2001) Impact of coronary artery remodeling on clinical presentation of coronary artery disease: an intravascular ultrasound study. *J Am Coll Cardiol* 37:63–69. doi:[10.1016/S0735-1097\(00\)01097-4](https://doi.org/10.1016/S0735-1097(00)01097-4)
9. Glagov S, Weisenberg E, Zarins CK et al (1987) Compensatory enlargement of human atherosclerotic coronary arteries. *N Engl J Med* 316:1371–1375
10. Schoenhagen P, Ziada KM, Kapadia SR et al (2000) Extent and direction of arterial remodeling in stable versus unstable coronary syndromes: an intravascular ultrasound study. *Circulation* 101:598–603
11. Coskun AU, Yeghiazarians Y, Kinlay S et al (2003) Reproducibility of coronary lumen, plaque, and vessel wall reconstruction and of endothelial shear stress measurements in vivo in humans. *Catheter Cardiovasc Interv* 60:67–78. doi:[10.1002/ccd.10594](https://doi.org/10.1002/ccd.10594)
12. Stone PH, Coskun AU, Kinlay S et al (2003) Effect of endothelial shear stress on the progression of coronary artery disease, vascular remodeling, and in-stent restenosis in humans: in vivo 6 months follow-up study. *Circulation* 108:438–444. doi:[10.1161/01.CIR.0000080882.35274.AD](https://doi.org/10.1161/01.CIR.0000080882.35274.AD)
13. Stone PH, Coskun AU, Kinlay S et al (2007) Regions of low endothelial shear stress are the sites where coronary plaque progresses and vascular remodeling occurs in humans: an in vivo serial study. *Eur Heart J* 28:705–710. doi:[10.1093/eurheartj/ehl575](https://doi.org/10.1093/eurheartj/ehl575)
14. Steigner ML, Otero HJ, Cai T et al (2009) Narrowing the phase window width in prospectively ECG-gated single heart beat 320-detector row coronary CT angiography. *Int J Cardiovasc Imaging* 25:85–90. doi:[10.1007/s10554-008-9347-8](https://doi.org/10.1007/s10554-008-9347-8)
15. Rybicki FJ, Otero HJ, Steigner ML et al (2008) Initial evaluation of coronary images from 320-detector row computed tomography. *Int J Cardiovasc Imaging* 24:535–546. doi:[10.1007/s10554-008-9308-2](https://doi.org/10.1007/s10554-008-9308-2)
16. Succi S (2001) *The Lattice Boltzmann equation*. The Oxford University Press, Oxford
17. Bernaschi M, Fatica M, Melchionna S et al (2008) A flexible high-performance Lattice Boltzmann GPU code for the simulations of fluid flows in complex geometries. *Comput Phys Commun* (submitted)
18. Stone PH, Coskun AU, Yeghiazarians Y et al (2003) Prediction of sites of coronary atherosclerosis progression: In vivo profiling of endothelial shear stress, lumen, and outer vessel wall characteristics to predict vascular behavior. *Curr Opin Cardiol* 18:458–470. doi:[10.1097/00001573-200311000-00007](https://doi.org/10.1097/00001573-200311000-00007)
19. Miller JM, Rochitte CE, Dewey M et al (2007) Late-breaking clinical trial abstracts from the American Heart Association's Scientific Sessions. *Circulation* 116:2630
20. Min J, Jollis J, Dowe D et al (2007) Assessment by coronary computed tomographic angiography of individuals undergoing invasive coronary angiography: results from the multicenter ACCURACY Trial (abstract SSE26-04). In: 94th scientific assembly and annual meeting of the radiological society of North America. Chicago, IL: 2007